Effect of temperature on current through various recombination channels in GaAs solar cells with GaInAs quantum dots

© M.A. Mintairov, V.V. Evstropov, S.A. Mintairov, R.A. Salii, A.M. Nadtochiy, N.A. Kalyuzhnyy

Ioffe Institute,
194021 St. Petersburg, Russia
E-mail: mamint@mail.ioffe.ru

Received June 7, 2023
Revised October 18, 2023
Accepted December 6, 2023

The influence of reducing carrier of thermal escape rate with temperature decreasing in various channels on the dark saturation current of a GaAs $p-n$ junction with $Ga_{0.8}In_{0.2}As$ quantum dots has been investigated. The dark saturation current has been calculated for temperatures ranging from 20 to 325 K. The calculation was based on the previously discovered current invariant, which determines the dependence of the saturation current on temperature and bandgap energy. The rates of recombination in various channels and their bandgaps were determined by photoluminescence spectra analysis. For various channels, characteristic temperatures were determined, below which thermal escape rate of carriers is practically absent. The saturation current calculation showed that, despite the change in the rate of recombination in different channels, it is determined only by the recombination in the channel with lower bandgap energy.

Keywords: solar cell, saturation current, current invariant, efficiency.

DOI: 10.61011/SC.2023.08.57624.5296

1. Introduction

One of the directions for increasing the efficiency (efficiency) of modern GaInP/GaAs/Ge multitransition (MT) solar cells (SC) is the use of quantum-sized objects (quantum wells, quantum dots, etc.) in subelements inside their $p-n$ transition) [1–16], i. e. objects with the excitonic nature of recombination-generation processes. Such objects ensure the absorption of photons with energies below the band gap of the subelement and the subsequent thermal release of electrons into the conduction band and holes into the valence band. As a result, free electron-hole pairs appear that can be separated by the electric field of the $p-n$ transition and, therefore, create a photovoltaic effect: increase the photogenerated current, which should lead to an increase in efficiency. However, the presence of quantum objects leads to the emergence of additional recombination channels, which increase the total saturation current of the $p-n$ transition [6,7] and, as a consequence, reduce the voltage generated by the subelement. The increase in saturation current is directly related to the energy of carrier recombination in quantum objects (QO) [6,7]. As shown earlier, the magnitude of the change in no-load voltage (dV_{oc}) is in practice equal to the difference between the band gaps of the $p-n$ transition ($E_{g,pn}$) and the quantum object ($E_{g,QO}$), $dV_{oc} \approx E_{g,pn}-E_{g,QO}$. This connection has been observed for all types of quantum objects.

For quantum wells (QW) this can be observed in works [8–11]. In the work, the authors, increasing the width of the well (from 1.5 to 5 nm), changed the effective value of its band gap $E_{g,QO}$ (from 1.3 to 1.16 eV). The $E_{g,QO}$ value was determined from both the photoluminescence peak and the absorption edge (data from measurements of the external EQE or internal IQE quantum efficiency). Samples with smaller $E_{g,QO}$ had lower no-load voltage (V_{oc}). The work [9] shows the spectral dependences of IQE for six samples with different numbers of QW. With an increase in the number of QW, the dark current density at the same voltage increased, which indicates that the saturation current increased, therefore, the voltage at the same currents decreased. In this case, the peak from the QW clearly shifted to longer wavelengths, indicating a corresponding decrease in $E_{g,QO}$. In works [10,11] devices using the technology of voltage balancing in the structure were studied: this approach promotes an increase in the no-load voltage of the SC, which is also accompanied by an increase in $E_{g,QO}$.

A similar correlation is observed for quantum dots [12–14]. In [12] the current-voltage curves, EQE dependences, and photoluminescence (PL) spectra are presented for samples with different quantum dots. The PL spectra contain the same number of peaks. For the two samples, the positions of the peaks with the lowest $E_{g,QO}$ do not differ (1030 and 1040 nm), which leads to the same value of V_{oc}. For the third sample, the peak position shifts significantly (1270 nm), leading to a corresponding drop in the no-load voltage (from 0.87 to 0.568 V). Other peaks are also observed in the PL spectra, but the voltage drop is caused by the shift of the peak with the lowest $E_{g,QO}$. In the work, an increase in the number of QD rows (up to 100 rows, when the emitter is strongly degraded) leads to a decrease inV_{oc} with a corresponding shift in the peak position by EQE towards longer wavelengths. Let us note that the peak positions of the two samples coincide, which corresponds to the same value V_{oc}.

Important data are presented in the work [14], where the EQE and electroluminescence spectra were compared for three different samples. The positions of the CT peaks characterizing the levels in QD and $E_{g,QO}$ differ slightly (in total, two peaks are observed 950 nm — 1.31 eV and 1050 nm — 1.18 eV), at In this case, for one of the samples the drop inV_{oc} is ~ 0.1 V greater. At the same time, for the same sample, the height of the high-energy peak (1.18 eV) is significantly lower than that of the lower-energy peak (1.31 eV). It follows from this that the rate of recombination through this level is higher, i. e., a larger number of carriers recombine through a level with lower energy. The difference between these energy levels is $(1.31-1.18)$ eV $= 0.13$ eV, which corresponds to the observed difference for the V_{oc} values (0.1 V). In other QO used in solar cells (quantum wires, QW and hybrid QO), there is also the indicated relationship [15,16].

Thus, firstly, in all SC with QO there is a strict relationship between the no-load voltage and $E_{g,QO}$. Secondly, the decrease V_{oc} is associated with an increase in the saturation current, which is determined by the rate of carrier recombination through various channels, including through a channel with an energy equal to $E_{g,QO}$. In this work, saturation currents are determined for various channels in SC with QW in a wide temperature range, as well as the rate and energy of recombination of all channels based on analysis of PL spectra. It was found that as the temperature decreases, recombination in the channels alternately saturates, but in the case of QD this does not lead to a significant improvement in the saturation current of the $p-n$ transition.

2. Object of study and description of the experiment

To study the photoluminescence spectra, a special double heterostructure was created, containing the same $In_{0.8}Ga_{0.2}$ As QD as in GaAs SC [16]. The heterostructure was grown by metal-organic gas-phase epitaxy in a setup with a horizontal reactor. For a detailed description of the technology, see [17]. In general, the heterostructure is an i-GaAs layer with a thickness of 500 nm, surrounded by two wide-gap barriers $Al_{0.3}Ga_{0.7}As$ with thicknesses of 250 and 50 nm, respectively. A single $In_{0.8}Ga_{0.2}As$ QD layer, grown in the Stranski–Krastanov mode with the formation of a wetting layer, is built into the center of the i-GaAs layer. As the optimal amount of material for the formation of QD, 2 monolayers of $In_{0.8}Ga_{0.2}As$ [17] were used.

To obtain PL spectra from experimental heterostructures containing QD, a Nd : YAG laser with a radiation wavelength of $\lambda = 532$ nm and a power of up to 350 mW was used as a radiation source. The sample radiation was focused at the entrance slit of an MDR-23 monochromator using a collecting lens. All measurements were carried out using a cooled Ge optical detector using a standard synchronous detection technique.

Saturation currents for solar cells were calculated using the approach described in the work [7]. When calculating the saturation currents of various recombination channels, the current invariant [18] was used. The contribution of each channel to the total saturation current (fraction) was estimated from the relative heights of the corresponding peaks in the PL spectra.

3. Main results

Some of the measured spectra are shown in Figure 1. The analysis showed that all spectra in the region from 1 to 1.4 eV include three ground peaks. The first peak (in the region of 1.35 eV) was clearly visible in the region of low temperatures and corresponds to the position of the well-like wetting layer. The second and third peaks corresponded to different types of QD. Both peaks are clearly distinguishable at high temperatures (> 250 K). At

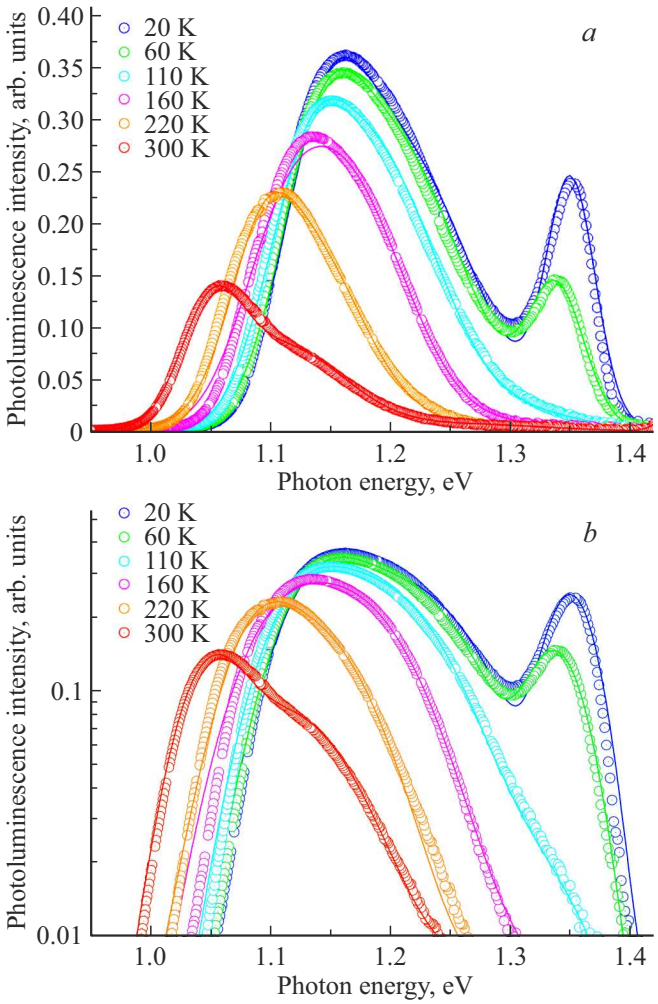

Figure 1. PL spectra on linear (a) and semilogarithmic (b) scales, measured in the temperature range 20–300 K (symbols — experimental data, solid lines — the result of approximation by the sum of three Gaussian peaks). (The colored version of the figure is available on-line).

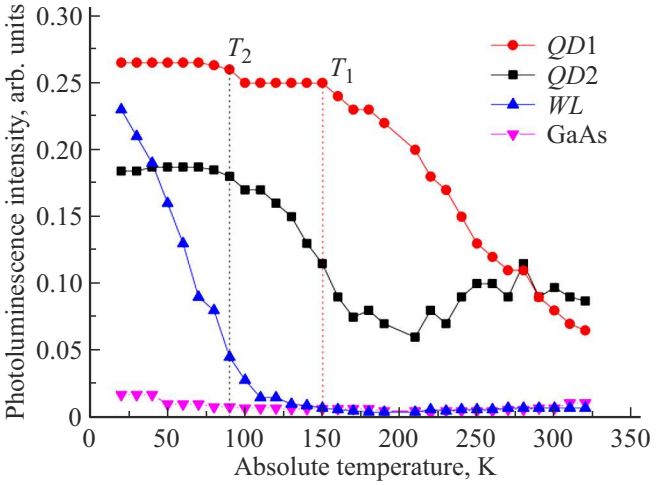

Figure 2. Temperature dependence of PL intensity for the wetting layer (blue triangles with the apex up) and QD of the first (red circles) and second (black squares) types. Vertical lines show characteristic temperatures for QD of the first (black line) and second (red line) types. (The colored version of the figure is available on-line).

a temperature of 300 K, there was the peak from the QD of the first type (QD1) in the region of 1.14 eV, and from the second type (QD2) — in the region of 1.05 eV. At low temperatures, a peak from the GaAs matrix also appeared in the spectra (at photon energies > 1.5 eV) (the peak had a small height and was poorly distinguished, therefore it is not shown in Figure 1).

All spectra were fitted by a function that included both the three main peaks and the peak from the GaAs matrix. The exclusion of the latter did not affect the results of the calculated spectral dependence. The results are shown in Figure 1 (lines). The performed approximation made it possible to isolate the spectra of individual channels (quantum dots of the first and second types, the wetting layer and the GaAs matrix) from the total PL spectrum. Figure 2 shows the dependence of the PL peak height for various recombination channels on temperature. It can be seen that three characteristic sections can be distinguished: from 20 to $T_1 = 90$ K, from T_1 to $T_2 = 150$ K and from 150 to 325 K. In the first section, the PL intensities of QD2 and QD1 practically do not change, which indicates the almost complete absence of thermal emissions of carriers in these quantum dots. In this case, with increasing temperature, there is a decrease in PL in the wetting layer. In the second section, the decrease in intensity in the wetting layer stops. As the temperature increases, carriers begin to leave points of the second type through thermal emissions. In the third section (at $T > T_2$), the rate of temperature emissions of carriers in QD1 increases; as a result, the departure of carriers with increasing temperature already affects the rate of recombination through QD1; the PL intensity from QD2 remains approximately constant. Thus, in the observed experiment, recombination processes in structures with QD were interrelated. The saturation of the recombination rate in one of the channels was accompanied by an increase (with a decrease in temperature) of the recombination rate in the other channel. Thus, the saturation of the recombination rate of carriers in KD1 corresponds to an increase in the recombination rate in the wetting layer. Also, at temperatures ~ 30 K, an increase in intensity through the GaAs matrix is visible, which possibly indicates the beginning of the process of saturation of the rate of carrier recombination in the wetting layer. Another interesting fact is that saturation of recombination at points of the first type begins at high temperatures, although their effective band gap is larger and, therefore, they have lower capture energies for electrons and holes. However, it is known that the density of QD1 is lower, and therefore recombination during current passage should mainly occur through „deeper“ QD2 [17]. It is possible that higher temperatures indicate a larger overall ejection/capture cross section. In this case, when using QD in solar cells, the ground attention is paid to current flow processes characterized by the magnitude of the saturation current. Therefore, in this work, special attention is paid specifically to the influence of the observed decrease (with a decrease in temperature) in the rate of thermal emissions of carriers on the saturation current of the $p-n$ transition.

4. Calculation of the saturation current of a GaAs solar cell with an $p-n$ transition GaInAs QD included in it

The calculation was carried out for a current with an ideality coefficient $A = 1$. This current is directly related to the rate of interband recombination and determines the maximum efficiency of the solar cell. The relative rate of such recombination in different channels can be determined by comparing the corresponding PL intensities (Figure 2). To calculate the saturation current, we used the assumption that the current invariant found in the work [18] is applicable to the quantum objects under consideration (wetting layer, QD1 and QD2). In accordance with [17] the saturation current is determined by the following expression:

$$J_0 = J_z \exp\left(-\frac{E_g}{kT}\right), \tag{1}$$

where J_z — current invariant, for GaInAs materials $J_z = 1 \cdot 10^4$ A/cm^2, k — Boltzmann constant, T — absolute temperature. To determine J_0 of each channel, the position of the corresponding PL peak was used as E_g. Thus, the temperature dependence of their saturation current was calculated for all channels (Figure 3). The following approach was used to determine the total saturation current. As is known [7], in the simplest case, the current-voltage characteristic of an $p-n$ transition with quantum objects (including QD) is described by a single exponential with a

pre-exponential factor equal to the saturation current J_0.

$$J = J_0 \exp\left(\frac{qV}{kT}\right). \quad (2)$$

Here q — electron charge, J — current through the $p-n$ transition, V — voltage. Let us note that expression (2) coincides in form with Shockley's formula [19]. However, the saturation current J_0 in this case includes additional terms due to recombination through QO. Accordingly, at a fixed voltage, the current of each channel is also described by (2). Obviously, the higher the contribution of each channel, the more carriers recombine in it. Accordingly, the greater the PL intensity in this channel. Therefore, from a comparison of the interband channel intensities, we can draw a conclusion about their contribution to the total current. Let us denote PL_i the PL intensity of the i-th channel, then, taking into account (1), the current in each channel will be determined by the following expression:

$$J_{0,i} = \frac{PL_i}{\Sigma PL_i} J_z \exp\left(-\frac{E_{g,i}}{kT}\right) = r_i J_z \exp\left(-\frac{E_{g,i}}{kT}\right), \quad (3)$$

where

$$r_i = \frac{PL_i}{\Sigma PL_i}$$

shows what part of the current flows through the i-th channel. Using (2), the total current through the $p-n$ transition is:

$$J = \sum J_{0,i} \exp\left(\frac{qV}{kT}\right). \quad (4)$$

From a comparison of (1) and (4) it is obvious that the total saturation current is determined by the following expression:

$$J_{0,\text{total}} = \sum J_{0,i} = \sum \left[r_i J_z \exp\left(-\frac{E_{g,i}}{kT}\right)\right]. \quad (5)$$

Using the spectra shown in Figure 2, the coefficients r_i for all 4 channels were determined for all temperatures. Using the saturation currents determined from (1) and the coefficients r_i in (5) allowed to calculate the total saturation current. The calculation results are shown in Figure 3. It can be seen that, despite the fact that with decreasing temperature, recombination begins to be determined not only by recombination in the QD, but also in the wetting layer, this does not lead to a significant decrease in the saturation current. This result was unexpected, i. e., the dominance of one of the recombination channels does not lead to the total saturation current approaching the saturation current of this channel. In fact, the total saturation current is always determined by the saturation current through channel KD2. This can be explained as follows. Let J_{01} be the maximum saturation current, let us express all saturation currents through it:

$$J_{0,i} = J_{0,1} \frac{J_{0,i}}{J_{0,1}} = J_{0,1} \frac{r_i J_z \exp\left(-\frac{E_{g,i}}{kT}\right)}{r_1 J_z \exp\left(-\frac{E_{g,1}}{kT}\right)}$$

$$= J_{0,1} \left(\frac{r_i}{r_1}\right) \exp\left(\frac{E_{g,1} - E_{g,i}}{kT}\right), \quad (6)$$

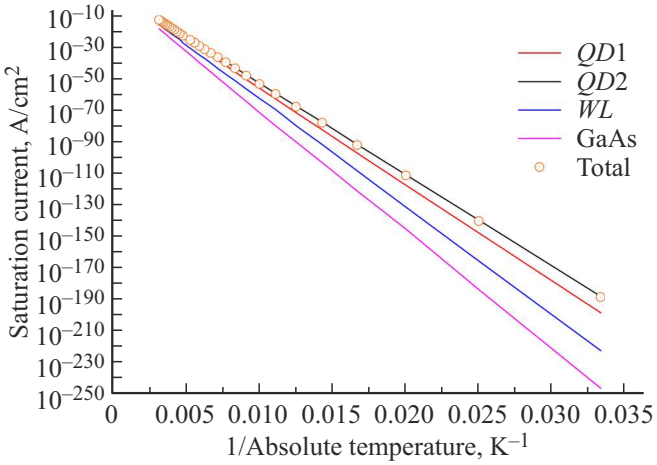

Figure 3. Temperature dependences of saturation current. Lines — various recombination channels in the GaAs $p-n$ transition with $Ga_{0.2}In_{0.8}As$ QD. Symbols — total saturation current.

if we substitute (1) into (5), taking into account (6) we get

$$J_{0,\text{total}} = \sum J_{0,i} = \sum_{i=1}^{n} J_{0,1} \left(\frac{r_i}{r_1}\right) \exp\left(\frac{E_{g,1} - E_{g,i}}{kT}\right)$$

$$= J_{0,1} + \sum_{i=2}^{n} J_{0,1} \left(\frac{r_i}{r_1}\right) \exp\left(\frac{E_{g,1} - E_{g,i}}{kT}\right). \quad (7)$$

In the experiment under consideration, the minimum difference in the energies of various channels was observed between QD2 and QD1 (Figure 1). For the entire temperature range it was ~ 0.1 eV. Therefore

$$\exp\left(\frac{E_{g,QD2} - E_{g,QD1}}{kT}\right) < 1/50.$$

As the temperature decreases, this ratio becomes even smaller. On the other hand, for all channels $\left(\frac{r_i}{r_1}\right) < 2$ (Figure 2), therefore in (7) the second term is always much smaller J_{01}, which is the reason that $J_{0,\text{total}} = J_{0,1}$. The above reasoning explains why in the case under consideration, despite the fact of the dominance of recombination through the channel in QD1 at temperatures < 250 K, the total saturation current is still determined by recombination in the channel QD2, which is caused by the large influence of the difference in recombination energies.

5. Conclusion

This work examines the temperature spectra of photoluminescence of $Ga_{0.8}In_{0.2}As$ quantum dots intended for use in $p-n$ transitions of solar cells. It was discovered that saturation of carrier recombination in quantum dots of the first type occurs at a temperature ($T \approx 150$ K) higher than that of quantum dots of the second type (90 K).

Saturation of carrier recombination in the wetting layer was not detected up to the temperature ~ 30 K, however, based on additional features (an increase in the photoluminescence intensity of the GaAs matrix), it was assumed that it begins in the temperature range 20–40 K. The temperature dependence of the saturation current of the GaAs $p-n$ transition, with $Ga_{0.8}In_{0.2}As$ quantum dots included in it, has been calculated. The saturation current of the $p-n$ transition is one of the basic parameters that determines the efficiency of solar cells created on its basis. It has been determined that despite the fact that the rate of radiative recombination in QD2 is less than the rate in QD1, and despite the saturation of the rate of recombination of carriers in QD2 and the increase in the recombination rate in the wetting layer, the saturation current is still determined only by recombination in QD2, which has the lowest energy recombination. Thus, when using $Ga_{0.8}In_{0.2}As$ QD in solar cells, the passage of current through their structure will be determined by the channels with the lowest recombination energy.

Conflict of interest

The authors declare that they have no conflict of interest.

References

[1] N.J. Ekins-Daukes, K.W.J. Barnham, J.P. Connolly, J.S. Roberts, J.C. Clark, G. Hill, M. Mazzer. Appl. Phys. Lett., **75** (26), 4195 (1999). DOI: 10.1063/1.125580

[2] B. Browne, J. Lacey, T. Tibbits, G. Bacchin, T.-C. Wu, J.Q. Liu, X. Chen, V. Rees, J. Tsai, J.-G. Werthen. AIP Conf. Proc., **1556**, 3 (2013) p. 3. DOI: 10.1063/1.4822185.

[3] D. Guimard, R. Morihara, D. Bordel, K. Tanabe, Y. Wakayama, M. Nishioka, Y. Arakawa. Appl. Phys. Lett., **96** (20), 203507 (2010). DOI: 10.1063/1.3427392

[4] V. Popescu, G. Bester, M.C. Hanna, A.G. Norman, A. Zunger. Phys. Rev. B, **78** (20), 205321 (2008). DOI: 10.1103/PhysRevB.78.205321

[5] S.A. Mintairov, N.A. Kalyuzhnyy, V.M. Lantratov, M.V. Maximov, A.M. Nadtochiy, S. Rouvimov, A.E. Zhukov. Nanotechnology, **26** (38), 385202 (2015). DOI: 10.1088/0957-4484/26/38/385202

[6] M.A. Mintairov, V.V. Evstropov, S.A. Mintairov, A.M. Nadtochiy, M.V. Nahimovich, R.A. Salii, M.Z. Shvarts, N.A. Kalyuzhnyy. Appl. Phys. Exp., **13** (7), 075002 (2020). DOI: 10.35848/1882-0786/ab9318

[7] M.A. Mintairov, V.V. Evstropov, S. A. Mintairov, A.M. Nadtochii, R.A. Salii, M.Z. Shvarts, N.A. Kalyuzhnyi. Techn. Phys. Lett., **46** (6), 599 (2020). DOI: 10.1134/S106378502006022X

[8] K. Toprasertpong, H. Fugii, T. Thomas, M. Fuhrer, D. Alonso-Alvarez, D.J. Farrell, K. Watanabe, Y. Okada, N.J. Ekins-Daukens, M. Sugiyama, Y. Nakano. Progr. Photovolt.: Res. Appl., **24** (4), 533 (2016). DOI: 10.1002/pip.2585

[9] D.B. Bushnell, N.D. Tibbits, K.W.J. Barnham, G.P. Connolly, M. Mazzer, N.J. Ekins-Daukes, J.S. Roberts, G. Hill, R. Airey. J. Appl. Phys., **97** (12), 124908 (2005). DOI: 10.1063/1.1946908

[10] R. Kellenbenz, W. Guter, P. Kailuweit, E. Oliva, F. Dimroth. *Proc. 8th Eur. Space Power Conf.* (4–19 September 2008, Constance, Germany).

[11] N. Ekins-Daukes. Solar Energy Mater. Solar Cells, **68** (1), 71 (2001). DOI: 10.1016/S0927-0248(00)00346-9

[12] D. Guimard, R. Morihara, D. Bordel, K. Tanabe, Y. Wakayama, M. Nishioka. Appl. Phys. Lett., **96** (20), 203507 (2010). May, 2010. DOI: 10.1063/1.3427392

[13] S.M. Hubbard, C. Plourde, Z. Bittner, C.G. Bailey, M. Harris, T. Bald, M. Bennett, D.V. Forbes, R. Raffaelle. In 2010 *35th IEEE Photovoltaic Specialists Conf.* (July 2010) p. 001217. DOI: 10.1109/PVSC.2010.5614053

[14] C.G. Bailey, D.V. Forbes, R.P. Raffaelle, S.M. Hubbard. Appl. Phys. Lett., **98** (16), 163105 (2011). DOI: 10.1063/1.3580765

[15] M. Sugiyama, H. Fujii, T. Katoh, K. Toprasertpong, H. Sodabanlu, K. Watanabe, D. Alonso-Álvarez, N.J. Ekins-Daukes, Y. Nakano. Progr. Photovolt.: Res. Appl., **24** (12), 1606 (2016). DOI: 10.1002/pip.2769

[16] M.A. Mintairov, V.V. Evstropov, S.A. Mintairov, M.V. Nakhimovich, M.Z. Shvarts, N.A. Kalyuzhnyy. AIP Conf. Proc., **2298**, 020007 (2020). DOI: 10.1063/5.0033763

[17] R.A. Salii, S.A. Mintairov, A.M. Nadtochiy, V.N. Nevedomskii, M.Z. Shvarts, N.A. Kalyuzhnyy. Semiconductors, **54** (10), 1267 (2020). DOI: 10.1134/S1063782620100255

[18] M.A. Mintairov, V.V. Evstropov, S.A. Mintairov, M.V. Nakhimovich, M.Z. Shvarts, N.A. Kalyuzhnyy. J. Phys.: Conf. Ser., **1697** (1), 012170 (2020). Dec. 2020. DOI: 10.1088/1742-6596/1697/1/012170

[19] W. Shockley. *The theory of p–n junctions in semiconductors and p–n junction transistors* (Bell System Techn. J., July 1949) p. 435.

Translated by Ego Translating